

Properties of hadronic interactions at $\approx 10^6$ GeV: Clues from cosmic-ray air showers

P. M. Fishbane*

Physics Department, University of Virginia, Charlottesville, Virginia 22901

T. K. Gaisser[†] and R. H. Maurer

Bartol Research Foundation of The Franklin Institute, Swarthmore, Pennsylvania 19081

J. S. Trefil*

Physics Department, University of Virginia, Charlottesville, Virginia 22901

(Received 26 November 1973)

We calculate the effect of intranuclear cascades and rising cross sections on the development of extensive air showers at energies up to 10^7 GeV. We find that these effects do not completely eliminate previously reported discrepancies between calculated and observed shower properties. We conclude that these discrepancies can only be removed by new features of high-energy interactions, predominantly heavy primaries at these energies, or both.

I. INTRODUCTION

In spite of the difficulties attendant to the collection of reliable cosmic-ray data, the range which the huge available incident energy affords makes pursuit of even the most rudimentary data worthwhile in any investigation of asymptotic phenomena. In particular, extensive air showers (EAS) are the result of a single incoming primary interacting with an air nucleus high in the atmosphere, and primary energies of 10^{15} – 10^{17} eV are not uncommon. At such high energies many particles are produced in the initial collision so that, in principle, many statistically reliable quantities and properties can be extracted from even a single event. Moreover, statistically significant numbers of showers are observed in this energy range.

It is possible to imagine that such events could provide both cosmological information from data on the composition of highly energetic primaries and information on high-energy phenomena themselves. Interpretation of the data is, however, complicated by the fact that properties of the EAS observed deep in the atmosphere are a consequence of a cascade involving many hadronic interactions. Thus, in practice, it is not yet possible to separate uniquely the cosmological and high-energy aspects. On the other hand, as Gaisser and Maurer¹ have emphasized, EAS provide the only opportunity for obtaining information from cosmic rays at $E \geq 10^5$ GeV on features of the central region in multiparticle production, such as multiplicity. This is to be contrasted with the observation of properties of uncorrelated cosmic rays, such as muon flux and μ^+/μ^- ratio,² which are sensitive primarily to the forward fragmentation region. The difference arises from the fact that

an EAS is the result of a single energetic primary, whereas uncorrelated cosmic-ray fluxes, arising from many primaries, reflect the steepness of the primary cosmic-ray spectrum.

There are many interesting ideas on high-energy reactions which are currently under consideration. One entire class of these would come under the heading of scaling models, in which inclusive experiments exhibit Feynman scaling. Such models are always characterized by a multiplicity of produced particles which grows logarithmically with the energy in hadron-hadron collisions. Another class of models (encompassing both statistical and hydrodynamical approaches) does not exhibit Feynman scaling and gives multiplicity growth as the $\frac{1}{4}$ power of energy. A third intriguing possibility is that total cross sections saturate the Froissart bound, i.e., grow as the squared logarithm of the energy. (In fact recent cosmic-ray results have heightened interest in this case.³⁻⁵) It is not clear whether the dynamics of such a limiting case allows for scaling behavior or not. These classifications are not meant to be complete or mutually exclusive. They are all hinted at or accommodated by present accelerator data, and in this paper we shall discuss the possibility of using EAS data to study these questions at very high energies. This work represents a continuation and extension of previous studies by Gaisser and Maurer.

A particular quantity which is measured in extensive air showers and which lends itself to tests of the asymptotic ideas above is the ratio of muons to electrons and positrons as a function of angle of shower axis, atmospheric depth (although most data come from sea level), and muon energy. A related quantity on which there are data is shower size as a function of atmospheric depth. (The

number of electrons and positrons is sometimes referred to as the shower size.) The detected electrons and positrons are degraded in energy at sea level, representing the remnants of electromagnetic showers which in turn are initiated by π^0 's. Because the electromagnetic component originates from π^0 's produced along the hadronic core of the shower, shower size deep in the atmosphere depends primarily on the fraction of energy given to π^0 's, and hence on energy of the shower primary, and on depth of penetration of the shower core into the atmosphere. In addition to obvious dependence on primary energy, penetration depth is related both to the elasticity of the leading hadron in π^\pm - or N -initiated interactions as well as to the size of hadron-interaction cross sections.

Muons, on the other hand, are the products of decaying π^\pm 's. Once produced they are relatively stable, and hence carry information about multiplicity in individual interactions at high energy.

On the basis of these features of EAS development, Gaisser and Maurer¹ suggested that the observed average μ/e ratio should be sensitive to differences between models of hadronic inter-

actions; in particular, to differences in energy dependence of average multiplicity. Although, as is well known, both $E^{1/4}$ and $\ln E$ give adequate representations of multiplicity through the CERN ISR energy range, the predictions of these two multiplicity laws are quite different at EAS energies. (See Fig. 1.) Thus it is reasonable to expect calculated EAS properties to reflect differences between assumed energy dependence of average multiplicity.

In their previous work, Gaisser and Maurer assumed Feynman scaling to hold with scaled inclusive cross sections taken from the ISR p - p data. They found large discrepancies between calculated and observed μ/e ratios and size-versus-depth data when the primary cosmic rays were assumed to be largely protons. The calculated μ/e ratio was too low, and the calculated showers penetrated much further into the atmosphere than is observed experimentally.

Although several authors^{6,7} have concluded from such discrepancies that Feynman scaling fails at the highest energies, we feel that the complexity of the data prevents one from drawing this conclusion as an immediate inference. In addition to

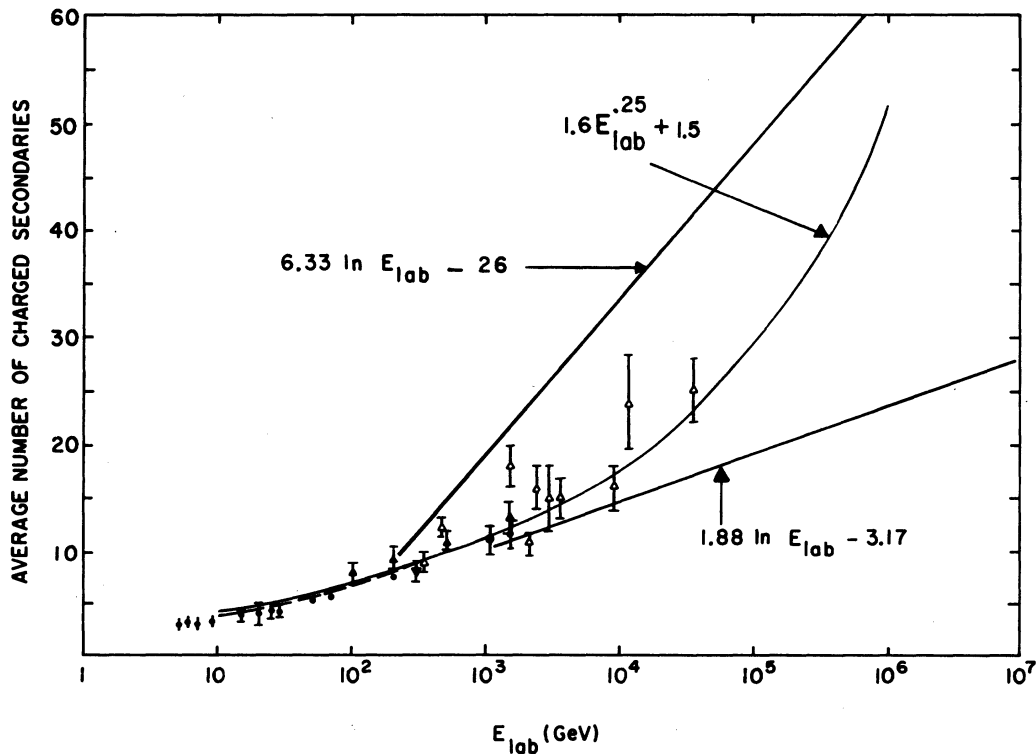


FIG. 1. Average number of charged secondaries in pp interactions vs E_{lab} . The lower logarithmic curve is the asymptotic form of the fit of Ref. 11. The curve $\propto E^{1/4}$ is a quarter-law fit to the data between 100 and 10^4 GeV. The highest curve is an approximate representation of the charged multiplicity in p -air collisions (neglecting target nucleon fragments) that comes from the intranuclear-cascade calculation reported here.

a possible breakdown of scaling at high energy, the following factors have been mentioned by Gaisser and Maurer as playing a possible role in the failure of the simple calculation described above: intranuclear cascading, increasing σ^T , and heavy primaries. It should be emphasized that all these possibilities operate in the same direction, namely, to make the shower develop faster and to increase μ/e , hence improving the agreement with the data. These effects can be understood as follows: Intranuclear cascading increases the multiplicity of secondaries in a given collision and tends to decrease the leading particle elasticity. An increasing p -air cross section (which arises as a consequence of an increasing p - p cross section) decreases the mean free path in air, thereby speeding up the development of the shower. Heavy primaries will have a similar effect because, crudely speaking, a primary nucleus of given total energy E and mass number A can be thought of as A particles of energy E/A whose individual showers are therefore less energetic and develop faster. Any mechanism which increases the number of pions tends to increase the number of muons, and hence the μ/e ratio. Since EAS are normally observed after the electromagnetic component has passed maximum, any mechanism which speeds up shower development will tend to decrease the calculated size at a fixed depth, and hence to increase the calculated μ/e ratio.

In this paper we report results of a calculation of EAS development that includes the effects of intranuclear cascading and of increasing $\sigma_{p\text{-air}}$. We find that including these effects, though it reduces the discrepancy between calculated and observed showers, still fails to account for the observed high μ/e ratio and rapid shower development.

Possible implications of these results are the following:

(1) Elementary particle interactions are qualitatively different at EAS energies from simple extrapolations of models which fit present data. In particular, such new physics might manifest itself in a mechanism which has the effect of depositing energy preferentially in the electromagnetic component of the shower⁸ (e.g., the appearance of heavy leptons). Alternatively, or additionally, one might have a radical breakdown of Feynman scaling, including the breakdown of scaling in the fragmentation region. Preliminary calculations by Gaisser *et al.*⁹ using the Landau hydrodynamical model, in which strong violations of scaling occur only near $x=0$, cannot account for the observed μ/e ratio and rapid shower development. On the contrary, a strong violation of scaling in the fragmentation region, corre-

sponding to a decrease in the "leading particle effect," seems to be required.

(2) The composition of the primary cosmic radiation at these energies may be heavy nuclei (e.g., iron).

We shall show that the combination of intranuclear cascading, increasing $\sigma_{p\text{-air}}$, and $A_{\text{eff}} \approx 50$ can account both for the observed μ/e ratio and the size versus depth measurements, a point emphasized recently by Gaisser *et al.*⁹ We stress, however, that further work is required to infer the relative importance of the possibilities mentioned above. In particular, a satisfactory picture of EAS development must also account for hadronic content of the shower, for lateral distributions of the various shower components, and for fluctuations of shower properties.

The organization of this paper is as follows: In Sec. II we review the development of an atmospheric shower. In Sec. III we review the Feynman scaling approach and discuss its incorporation with Glauber theory to give appropriate distribution for nuclear targets. We also discuss the inclusion of rising total cross sections. Section IV contains a presentation of results and discussion.

II. ATMOSPHERIC SHOWER DEVELOPMENT

Atmospheric cascades produced by primary cosmic rays of total energy $\geq 10^5$ GeV penetrate far enough so that the shower front can be observed deep in the atmosphere, at sea level or mountain altitude. Development of a shower in the atmosphere, and hence its structure at the observation level, depends, on the one hand, on properties of the atmosphere and on properties of electromagnetic and weak interactions that are well understood (e.g., electromagnetic cascading via alternate pair production and bremsstrahlung and the π - μ - e decay) and, on the other hand, on properties of hadronic interactions, which are essentially unknown above $\sim 10^4$ GeV and for which some model must be assumed. We first show how the hadronic core of the shower is calculated. We then describe how the known features of weak and electromagnetic interactions are used to compute the muon and electromagnetic shower components, which are secondary to the hadronic component.

The following coupled integro-differential equations govern the hadronic cascade:

$$\frac{dN_{E_0}(e, y)}{dy} = -\frac{N_{E_0}(E, y)}{\lambda_N(E)} + \int_E^\infty \frac{\bar{F}_{NN}(E, E')}{E} \frac{N_{E_0}(E', y)}{\lambda_N(E')} dE' \quad (2.1)$$

and

$$\begin{aligned} \frac{d\pi_{E_0}(E, y)}{dy} = & -\pi_{E_0}(E, y) \left(\frac{1}{\lambda_\pi(E)} + \frac{\epsilon_\pi}{Ey \cos \theta} \right) \\ & + \int_E^\infty \frac{\bar{F}_{N\pi}(E, E')}{E} \frac{N_{E_0}(E', y)}{\lambda_N(E')} dE' \\ & + \int_E^\infty \frac{\bar{F}_{\pi\pi}(E, E')}{E} \frac{\pi_{E_0}(E', y)}{\lambda_\pi(E')} dE', \end{aligned} \quad (2.2)$$

where $\pi_{E_0}(E, y)dE$ and $N_{E_0}(E, y)dE$ are respectively the numbers of nucleons and of charged pions at atmospheric depth y (in g/cm^2) and energy between E and $E+dE$ due to a primary nucleon of energy E_0 , and $\lambda_\pi(E)$ and $\lambda_N(E)$ are the pion and proton interaction length in air. (The latter are taken to be energy-dependent to reflect the possible energy dependence of the p -air and π -air cross section.) The quantity $\epsilon_\pi dy/Ey \cos \theta$ is the probability that a pion along the shower axis with zenith angle θ decays in dy ($\epsilon_\pi \equiv h_0 m_\pi / \tau_0 \cong 128$ GeV, where τ_0 is the pion lifetime and m_π its mass). The form of this term assumes a simple exponential atmosphere¹⁰ with scale height h_0 (≈ 7 km).

The quantities \bar{F}_{AB} in Eqs. (2.1) and (2.2) carry the information on hadronic production; they are inclusive cross sections integrated over transverse momentum and normalized to the p -air inelastic cross section. Thus

$$\bar{F}_{AB}(E, E') \approx E \frac{dN_{AB}(E, E')}{dE}, \quad (2.3)$$

where $dN_{AB}(E, E')$ is the number of B particles produced with lab energy between E and $E+dE$ in the collision of an A particle of lab energy E' with an air nucleus. The derivation of these quantities from the more fundamental cross sections on single nucleon targets is described in Sec. III.

It is clear that the cascade equations as written include only nucleons and charged pions. (π^0 s always decay before interacting and thus contribute only to the electromagnetic cascade.) Separate treatment of other species would require further coupled equations; therefore, we have for simplicity treated kaons as pions and strange baryons as nucleons. This should be a reasonable procedure since $K/\pi \sim 0.1$,¹¹ since $\frac{2}{3}$ of the charged kaons have the same $\mu\nu$ decay mode as π^\pm , and since kaon-initiated hadronic interactions are similar to those of pions. We have also neglected $N\bar{N}$ production. Indications are^{11,12} that the $N\bar{N}/\pi$ ratio becomes fairly large at high energies, perhaps approaching 15–20% asymptotically. This, therefore, will not be a good approximation for computing the fluxes of moderate-energy (20–1000 GeV) hadrons in the shower. It

is, however, expected to be a reasonable first approximation for computing the electromagnetic and muon components of the shower. (Grieder¹³ has pointed out that an appreciable fraction of $N\bar{N}$ production may affect the cascade development significantly, including an increase in the μ/e ratio at low muon energies, a change that goes in the direction of improving agreement between calculated and observed showers. The increase in low-energy muons is due to enhanced production of low-energy π^\pm deep in the atmosphere due to the ability of moderate energy $N\bar{N}$ pairs to penetrate the atmosphere without decay. Grieder finds an increase of a factor of four or five in μ/e at $E_\mu \sim 1$ GeV using a high-multiplicity model for pion production and putting about 9% of the interaction energy into $N\bar{N}$ production. The data indicate,¹⁴ however, that the fraction of energy going into $N\bar{N}$ production asymptotically is more like 3%. In addition, a scaling-type model produces fewer pions. Indication of a calculation without intranuclear cascading⁹ is that the μ/e ratio is enhanced by $\sim 40\%$ at $E_\mu \sim 1$ GeV. Because of increased multiplicity due to intranuclear cascading this will be increased somewhat, but the conclusions reached here without $N\bar{N}$ production are not expected to be altered unless $N\bar{N}$ production becomes asymptotically more important than suggested, for example, by the parametrization of Ref. 14. Nevertheless, this point remains to be investigated fully, and an unexpectedly large further increase in $N\bar{N}$ production beyond ISR energies would make a significant contribution toward removing the discrepancy between calculated and observed EAS properties.)

Finally, we are also able to neglect nucleons that are target fragments, as they remain at low enough energies in the lab not to contribute to shower development. With these assumptions concerning nucleon production each shower contains exactly one core nucleon, the degraded primary.

The solutions of Eqs. (2.1) and (2.2) subject to the power-law boundary condition, $N(E, 0) = KE^{-\gamma}$ = primary cosmic-ray spectrum, have been discussed in the context of scaling by Frazer *et al.*¹⁵ and by many others recently, in particular, in calculations of muon flux and the μ^+/μ^- ratio. These solutions may be obtained analytically (for $E_\pi > 100$ GeV), provided Feynman scaling holds in the forward fragmentation region (i.e., assuming limiting fragmentation). Conversely, properties of uncorrelated cosmic rays, such as μ^+/μ^- , are sensitive only to the forward fragmentation region; hence calculations of such properties test limiting fragmentation only and not Feynman scaling near $x=0$. As mentioned in the Introduc-

tion this is a consequence of the steep primary spectrum ($\gamma \cong 2.7$), which suppresses the effects of secondaries which do not carry off a finite fraction of the primary energy as $E \rightarrow \infty$.

For the EAS problem, on the other hand, one must solve the cascade equation subject to $\pi_{E_0}(E, 0) = 0$ and $N_{E_0}(E, 0) = \delta(E - E_0)$, corresponding to a single primary nucleon. In this case shower properties are sensitive both to the central region and to the forward fragmentation region, but the solutions must be obtained numerically. An additional simplification can be achieved as a consequence of two further approximations: (1) The nucleon interaction length is approximated by a constant, say, $\lambda_N(E) \sim \lambda_N(\frac{1}{2}E_0)$. [This should

be reasonable since $\lambda_N(E)$ is slowly varying, since the approximation is made only for one hadron in the shower, and since λ_N is correct near the beginning of the cascade where the core nucleon is most energetic and thus most effective in generating the cascade.] (2) Limiting fragmentation is assumed to hold for F_{NN} and it is approximated by a function of the form

$$F_{NN}(E, E') = \alpha(E/E')^\alpha. \quad (2.4)$$

[The form (2.4) is a good approximation to the ISR and NAL $NN \rightarrow N+X$ data, with $\alpha \sim 1$ corresponding to a nucleon elasticity $= \alpha/(\alpha+1) \sim \frac{1}{2}$.¹⁶]

With these approximations the solution to Eq. (2.1) can be obtained explicitly. It is¹⁷

$$N_{E_0}(E, y) = \frac{1}{E_0} e^{-y/\lambda_N} \left\{ \delta(1 - E/E_0) + \left(\frac{E}{E_0}\right)^{\alpha-1} \left(\frac{\alpha y}{\lambda_N \ln(E_0/E)}\right)^{1/2} I_1 \left(2 \left[\frac{\alpha y \ln(E_0/E)}{\lambda_N} \right]^{1/2} \right) \right\}. \quad (2.5)$$

The remaining Eq. (2.2) has been solved numerically by a modified method of successive generations as in the previous work of Gaisser and Maurer.¹

The electromagnetic component of the shower is calculated in a straightforward way from the solutions of Eqs. (2.1) and (2.2). We have for the average number of electrons and positrons at depth y_0 in a shower of primary energy E_0

$$\mathcal{N}(E_0, y_0) = \int_0^{y_0} dy \int_0^{E_0} dW \frac{S(W, y_0 - y)}{W} \times \int_w^{E_0} dE' G_{E_0}(W, y, E'), \quad (2.6)$$

where

$$G_{E_0}(W, y, E') = \frac{\bar{F}_{N\gamma}(W, E') N_{E_0}(E', y)}{\lambda_N(E')} + \frac{\bar{F}_{\pi\gamma}(W, E') \pi_{E_0}(E', y)}{\lambda_\pi(E')} \quad (2.7)$$

The quantity $S(W, y_0 - y)$ is the number of electrons and positrons at depth y_0 due to a photon produced at y with energy W . It can be represented by the analytic form¹⁸

$$S(W, y) = \frac{0.31}{\sqrt{\beta}} e^{t[1 - (3/2) \ln r]}, \quad (2.8)$$

where $t = y/l_{\text{air}}$ is the atmospheric depth measured in radiation lengths, $l_{\text{air}} \cong 37.7 \text{ g/cm}^2$; $\beta = \ln(W/e_c)$, $e_c = 0.0842 \text{ GeV}$, and $r = 3t/(t+2\beta)$.

We have made the conventional assumptions that the electromagnetic cascade comes entirely from photons from π_0 decay; specifically, that for incident hadrons h ,

$$\bar{F}_{h\gamma}(W, E) = \bar{F}_{h\pi^0}(\frac{4}{3}W, E) + \bar{F}_{h\pi^0}(4W, E). \quad (2.9)$$

Motivated by charge independence, we assume the π^0 distributions to be the average of the π^+ and the π^- distributions [see Eqs. (3.7)–(3.12) in Sec. III]. This set of assumptions is of fundamental importance for the results we obtain. If, for example, some new process operates at EAS energies by which energetic photons or electrons are produced directly in very-high-energy hadronic interactions, with a concomitant decrease in the energy fraction carried away by the produced pions, then the electromagnetic component of the shower will develop more rapidly in the atmosphere, reaching a maximum sooner and dying away more quickly.

To complete our calculation of shower properties we have only to calculate the integral muon number $N_\mu (> E_\mu)$ from $\pi_{E_0}(E, y)$. This has been done in a straightforward way, taking into account muon decay and energy loss, in the manner described by Pal and Peters.¹⁹

The limited nature of the EAS calculation described above should be emphasized. We have calculated only linear shower development of average showers. Thus a large fraction of available air-shower data (that on fluctuations and lateral distributions of the various shower components) has not been used here to help elucidate features of hadronic interactions at these very high energies. In addition, the neglect of NN production limits the accuracy of the calculated moderate-energy hadronic fluxes. Calculation of total electron and muon fluxes is, however, sufficient to study the magnitude of the effects on shower development of intranuclear cascading and energy-dependent cross sections.

The limitations described above present two practical difficulties for comparing calculated with observed shower properties. First, computed values of total electromagnetic shower size and of total muon number must be compared with the corresponding numbers quoted by air-shower experimenters. These quantities are not, however, directly measured. They must be constructed for each shower by fitting the observed densities of particles in the detectors that comprise the air-shower array to a semiempirical lateral-distribution function. The integrated showers are then put into bins (usually according to shower size) and average properties calculated for each bin. This process involves obvious difficulties, and the use of different procedures for different experiments is presumably a source of systematic error. We have made no attempt to remove such systematic errors, but have taken the integrated, averaged data as quoted by various authors.

The second difficulty is a consequence of the fact that the shower properties are averaged for showers in the same size bin (showers of fixed size), whereas the computation produces properties averaged over showers with the same primary energy (showers of fixed energy). The relation between primary energy and shower size at fixed depth is different in the two cases. For showers of fixed size, N_e , the steep primary spectrum favors fluctuations that produce a given size with unusually low primary energy relative to the fixed-energy case. Thus for $\mathcal{N} = \langle N_e \rangle_{E_0} = N_e$, E_0 is higher than $\langle E_0 \rangle_{N_e}$. Important causes of this effect are fluctuations in depth of first interaction and fluctuations in the energy fraction carried off by produced π^0 's in early interactions.

Since we calculate only average shower properties we can compute the relation between E_0 and \mathcal{N} (showers of fixed energy) but not the relation between N_e and $\langle E_0 \rangle_{N_e}$ for showers of fixed size. De Beer *et al.*²⁰ have calculated both relations using, however, a phenomenological model²¹ for the production cross sections that is appropriate only for the $\lesssim 30$ GeV energy range. Since the over-all account of shower properties as given by their calculation is reasonable, we have taken $N_e / \langle N_e \rangle_{E_0}$ at $E_0 = \langle E_0 \rangle_{N_e}$ from their calculation and used our result for the relation between $\langle N_e \rangle_{E_0}$ and E_0 for showers of fixed energy to find $\langle E_0 \rangle_{N_e}$ for showers of fixed size, N_e . This is the same procedure used in the earlier work of Gaisser and Maurer¹ and of Gaisser *et al.*⁹ (Use of the fixed E_0 relation between E_0 and \mathcal{N} would lead to about a factor-of-two increase in N_μ / N_e . This sets the absolute upper limit on possible error due to our method of computing the relation between $\langle E_0 \rangle_{N_e}$ and N_e , and a realistic estimate of the uncertainty

would be much less than this.)

We emphasize that this procedure is necessary only for computing N_μ / N_e . The fixed-size difficulty does not exist for the comparison between calculated and observed size-versus-depth curves. This is because the size-versus-depth curves are established²² by taking cuts of constant intensity in the integral size spectrum of showers with different zenith angles. Since the depth of material penetrated by a shower is $y_{\text{vertical}} \sec \theta$, and since showers of the same frequency are from primaries of the same energy, this establishes a size-versus-depth curve for showers of fixed energy for $y \geq y_{\text{vertical}}$.

III. SCALING FUNCTIONS

It remains for us to specify the functions \bar{F}_{AB} , which are inclusive single-particle cross sections on nuclear targets. These functions can in turn be determined in principle from single-particle distributions on nucleon targets if certain information on space-time characteristics of such a collision is available. We shall return to the nature of this information below, but for now we remark that the nuclear scattering distribution can be determined in practice only when the nucleon scattering distribution obeys Feynman scaling.

Therefore we remind the reader of the salient features of the scaling phenomenon. The experimental quantity of interest is the single-particle inclusive cross-section for the process $a + b \rightarrow c + X$. This quantity depends on three invariants, which can be chosen as in the definition

$$E_c \frac{d\sigma}{d^3p_c} = f(x, p_\perp^2, s), \quad (3.1)$$

where

$$x = p_\parallel^{c.m.} / p_\parallel^{\text{max.}} \xrightarrow{s \rightarrow \infty} 2p_\parallel^{c.m.} / \sqrt{s}.$$

The function f characteristically falls off rapidly for large p_\perp^2 , and the statement of Feynman scaling requires that

$$f(x, p_\perp^2, s) \xrightarrow{s \rightarrow \infty} f(x, p_\perp^2). \quad (3.2)$$

The regions $x > 0$, $x < 0$, and $x = 0$ are called the projectile-fragmentation, target-fragmentation, and pionization regions. While scaling is verified with good accuracy for the fragmentation regions, it is not yet clear whether a limit has been reached near $x = 0$ at ISR energies. This is, of course, one of the questions we hope to investigate in this study. The multiplicity of the produced particle c can be determined from the inclusive cross section,²³

$$\langle n_c \rangle = F(0, s) \ln[s / (\bar{\mu}_\perp^2)] - \text{const} + O(\bar{\mu}_\perp^2 / s^{1/2}), \quad (3.3)$$

where

$$F(x, s) = \frac{1}{\sigma_{\text{inel}}^{\text{ab}}} \int d^2p_{\perp} f(x, p_{\perp}^2, s) \quad (3.4)$$

and $\bar{\mu}_{\perp}^2 = \bar{p}_{\perp}^2 + m_c^2$, where \bar{p}_{\perp}^2 is the characteristic transverse momentum cutoff. Logarithmic growth in the expression for $\langle n_c \rangle$ is simply a phase-space effect in the "volume" variable rapidity, defined by

$$r_{\text{lab}} = \sinh^{-1}(p_{\parallel} / \mu_{\perp}).$$

Thus, logarithmic growth of multiplicity can be expected whenever F scales (and is therefore independent of s).

It is instructive to compare this multiplicity growth with that predicted by the Landau hydrodynamical model, in which F grows with s . This model predicts a multiplicity which grows as $E^{1/4}$. While such a difference would be apparent at asymptotic energies, Fig. 1 shows that current accelerators have not yet brought us to the asymptotic region in this respect.

In order to find the scaling functions on nuclear targets, we shall have to know the scaling functions for several reactions which can take place on the constituent nucleons. In particular, we shall need to know the distributions for the reactions

$$(i) \quad N + N \rightarrow \pi + X$$

and

$$(ii) \quad \pi + N \rightarrow \pi + X.$$

Since there are many more pions than nucleons produced in individual collisions, we shall neglect processes in which final-state nucleons are produced by incident pions on nucleons in working through the nuclear cascade (although these processes *are* included in considerations of energy conservation—see below). Numerical estimates show that this is not an important approximation for calculation, and it clearly would be possible to include final-state nucleon effects if it were thought to be necessary. As long as energy conservation is enforced, distinction among different types of hadrons is unnecessary for the intranuclear cascade as it is purely hadronic. It should also be noted that the pions in reactions (i) and (ii) can be of any charge since the lifetime of the π^0 is much greater than the nuclear radius. Thus, neutral pions participate directly in the intranuclear hadronic cascade, but contribute only indirectly (via the intranuclear cascade) to the atmospheric hadronic cascade.

Before we give the required scaling functions in more detail, let us discuss some qualitative aspects of the nuclear cascade calculation. As discussed elsewhere,²⁴ for purposes of this calculation multiparticle production models can be divided into two major classes (see Fig. 2). In the first

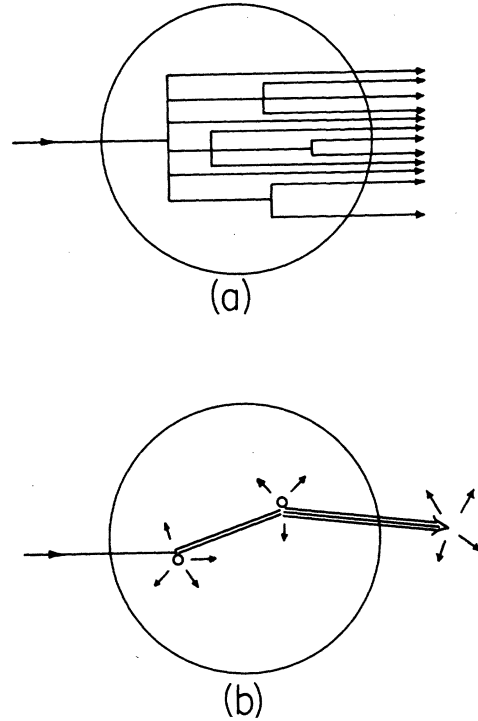


FIG. 2. (a) Schematic picture of nuclear cascade in incoherent-production models. (b) Schematic picture of the production chain in coherent-production models.

class, coherent-production models (CPM),²⁵ the multiparticle final state can be regarded as the decay product of excited hadronic matter. This matter has a typically hadronic cross section and the decay time must be long compared to the nuclear radius. In these models it is the (unknown) scattering properties of the excited matter which come into play; plausible guesses for properties of the excited hadronic matter give nuclear-target properties which differ by $O(A^{1/3})$ from the corresponding nucleon-target properties. In the second class, incoherent-production models (IPM),²⁶ the complete multiparticle final state appears in a time short compared to the nuclear radius. These particles can rescatter independently within the nucleus, rapidly building up a cascade. In the IPM the multiplicity of particles contributing to the air-shower development builds up more quickly than in the CPM at the energies of interest. Therefore, of these two classes of models, the IPM will give an upper bound to the μ/e ratio, and we shall concentrate on this case. Clearly for IPM the single-particle distributions for reactions (i) and (ii) are directly relevant.

The scaling distributions F_{pp} , F_{pn} , $F_{p\pi\pm}$, and $F_{\pi\pm\pi\pm}$ are all measurable at accelerator energies for proton targets. We shall express the distributions which we require in terms of these measur-

able quantities by using (1) the energy-momentum conservation sum rule, (2) charge independence, and (3) factorization, by which we mean that the distributions in the projectile-fragmentation and pionization regions are independent of the target.

Charge independence motivates the assumption that particles in the pionization and projectile-fragmentation regions are independent of whether the projectile is a neutron or proton. (Charge reflection relates final states.) By energy conservation

$$\int_0^1 \sum_r F_{pr} dx = 1$$

$$\approx \int_0^1 (F_{pp} + F_{pn} + F_{p\pi^+} + F_{p\pi^-} + F_{p\pi^0}) dx, \quad (3.5)$$

where we remind the reader that we are here treating kaons and $N\bar{V}$'s as pions. This means that the $F_{p\pi}$ in Eq. (3.5) must be scaled up from the measured values to account for kaon production. This is done by noting the nucleon elasticity is given by¹⁶

$$\eta = \int_0^1 (F_{pp} + F_{pn}) dx \approx 0.5. \quad (3.6)$$

Equation (3.6) is then used to scale up the values of the $F_{p\pi}$ by multiplication by a constant factor. As expected, this factor gives a 10% increase, since kaon production is 10% of pion production.

Charge independence also motivates our treatment of π^0 's both as produced particles and as projectiles. This assumption is also supported by measured values of $p + p \rightarrow \gamma + X$ and $\pi^\pm + p \rightarrow \gamma + X$ under the assumption that all photons are π^0 decay products. We choose

$$F_{N\pi^0} \approx F_{p\pi^0} \approx \frac{1}{2}(F_{p\pi^+} + F_{p\pi^-}). \quad (3.7)$$

This gives us for the required reaction (i), $N+N \rightarrow \pi+X$, a total distribution

$$F_{N\pi} = \frac{1}{2}(F_{p\pi^+} + F_{p\pi^-} + F_{p\pi^0} + F_{n\pi^+} + F_{n\pi^-} + F_{n\pi^0})$$

$$\approx \frac{3}{2}(F_{p\pi^+} + F_{p\pi^-}), \quad (3.8)$$

For pion production by pion projectiles, it is convenient to define the (measurable) cross section for production of charged pions by charged pions,

$$F_{\pi^c\pi^c} = \frac{1}{2}(F_{\pi^+\pi^+} + F_{\pi^+\pi^-} + F_{\pi^-\pi^+} + F_{\pi^-\pi^-}). \quad (3.9)$$

We then assume that

$$F_{\pi^c\pi^0} = \frac{1}{2}(F_{\pi^+\pi^0} + F_{\pi^-\pi^0})$$

$$\approx \frac{1}{2}F_{\pi^c\pi^c} \quad (3.10)$$

$$F_{\pi^0\pi^c} = F_{\pi^0\pi^+} + F_{\pi^0\pi^-}$$

$$\approx F_{\pi^c\pi^c} \quad (3.11)$$

and

$$F_{\pi^0\pi^0} \approx \frac{1}{2}(F_{\pi^+\pi^+} + F_{\pi^-\pi^-}). \quad (3.12)$$

This gives us for the required reaction (ii), $\pi+N \rightarrow \pi+X$, a total distribution

$$F_{\pi\pi} = \frac{1}{3}(F_{\pi^+\pi^+} + F_{\pi^+\pi^0} + F_{\pi^+\pi^-} + F_{\pi^0\pi^+} + F_{\pi^0\pi^0}$$

$$+ F_{\pi^0\pi^-} + F_{\pi^-\pi^+} + F_{\pi^-\pi^0} + F_{\pi^-\pi^-})$$

$$\approx \frac{4}{3}F_{\pi^c\pi^c} + \frac{1}{6}(F_{\pi^+\pi^+} + F_{\pi^-\pi^-}). \quad (3.13)$$

Equations (3.13) and (3.8) are then used as input for the nuclear-cascade calculation. This calculation, which has been discussed in detail elsewhere,²⁶ uses a multiparticle generalization of the Glauber theory to produce single-particle distributions \bar{F} on nuclear targets; at the energies of interest the output functions do not scale, even though the input functions are assumed to. For the output pions we assume that, for the atmospheric-shower calculations described in Sec. II, $\frac{2}{3}$ of the pions are charged and $\frac{1}{3}$ are neutral, independent of x . The distribution $\bar{F}_{N\pi} \equiv \bar{F}_{N\pi^\pm}(E, E_0)$ is displayed in Fig. 3 for $100 \text{ GeV} \leq E_0 \leq 10^8 \text{ GeV}$. The corresponding input scaling functions are shown by the dashed lines, and the data at 1000 GeV are taken from a summary of ISR data of Antinucci *et al.*¹¹ at $p_\perp = 0.4 \text{ GeV}$. (Throughout this calculation in all Lorentz transformations and transformations between y_{lab} and x we have taken the produced pions to have a fixed transverse mass of 0.41 GeV.)

The shower calculation also requires the nucleon elasticity $\bar{\eta}$ on nuclear targets [cf. Eqs. (2.4) and (2.5)]. The nature of the nuclear-cascade calculation makes it most convenient to extract this quantity by using energy conservation, Eq. (3.5),

$$\bar{\eta} = 1 - \int_0^1 \bar{F}_{N\pi} dx. \quad (3.14)$$

While $\bar{\eta} < \eta$ in general, we should state here that multiparticle propagation in nuclei is poorly described by a mean-free-path approximation. We have found that effects which might partially be described as self-shielding effects in the multipion final state are important. In fact, for a fixed multiplicity in the elementary interaction at the energies of interest, the output nuclear distribution is essentially independent of any increases in the elementary total cross sections. This happens because, while the mean free path for single-particle propagation would decrease with increasing σ_T , the shielding effects mentioned above also increase such that there is an approximate cancellation.

Numerically it is found that $\bar{\eta}$ decreases slowly with increasing energy, from ~ 0.4 at 10^3 GeV to ~ 0.3 at 10^8 GeV . This decrease is associated with

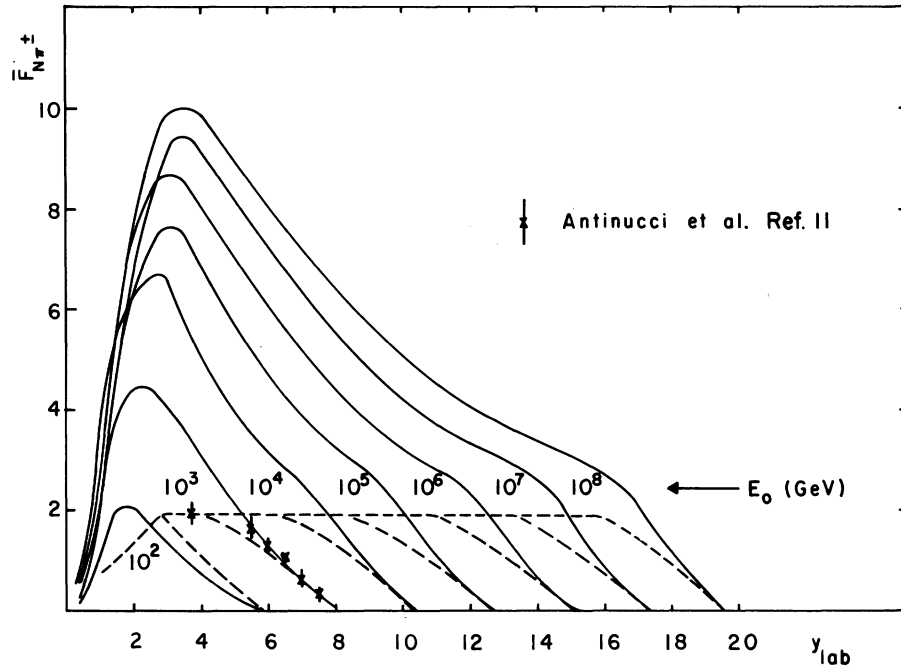


FIG. 3. Inclusive number distribution (integrated over transverse momentum) for charged pions produced in p -air collisions according to the IPM picture used here (solid lines) vs pion lab rapidity. The input scaling distributions off nucleon targets (dashed lines) are shown for comparison.

the shoulder observable in $\bar{F}_{N_{\pi}}$ in Fig. 3 that becomes more prominent with increasing energy. The shoulder is an artifact of the numerical methods used in computing the intranuclear cascade; the elasticity calculated with the shoulder removed is fairly constant above 1000 GeV and is only a few percent smaller than the input, nucleon-nucleon elasticity of 0.5. Nevertheless, in keeping with our attempt to seek an upper bound for the effect of intranuclear cascading on the μ/e ratio, we have used $\bar{\eta}=0.3$ throughout for the nucleon elasticity on nuclear targets. In those shower calculations presented here and earlier,^{1,9} which do not include intranuclear cascading, we have used a nucleon elasticity of 0.5.

We should also like to comment on the fact that the nuclear-cascade calculation proceeds under the assumption of input distributions which scale. In fact, input distributions increase with s from AGS to ISR energies by a large amount near $x=0$. In principle, the lower-energy components of the nuclear cascade should use the smaller single-particle distribution. However, by using the larger distribution throughout the calculation, one overestimates the output distribution and therefore the multiplicity and the μ/e ratio. This also is consistent with our approach of seeking an upper bound for the μ/e ratio, as is our use of IPM rather than CPM.

IV. RESULTS

To test the scaling model including intranuclear cascading we take the $F_{p,\pi^{\pm}}$ quantities from the results of ISR experiments at $s \approx 2600$ GeV². These scaling functions are about twice as large as those at AGS energies near $x=0$. If we write the AGS scaling function as $F_{p,\pi^{\pm}}^{\text{AGS}}(x)$, then the result can be reasonably approximated as $F^{\text{AGS}}(x) + F^{\text{AGS}}(5x)$. The distribution F_{π^+c,π^-c} is, of course, not measured at the ISR. However, in view of the recently observed²⁷ similarity between pion- and proton-initiated reactions at the NAL we also take $F_{\pi^+c,\pi^-c}(x) = F_{\pi^+c,\pi^-c}^{\text{AGS}}(x) + F_{\pi^+c,\pi^-c}^{\text{AGS}}(5x)$. These functions are then put through the intranuclear cascade under the IPM assumption, as discussed in Sec. III. The resulting nucleon elasticity becomes ~ 0.3 . These distributions are in turn put through the air-shower equations as described in Sec. II. From the resulting pion and nucleon flux we then calculate the muon flux and the flux of electrons and positrons. The resulting ratio of integral muon flux to total electromagnetic shower size for showers of fixed size $= 10^6$ is shown in Fig. 4. In the same figure are plotted results of the same calculation without nuclear cascade (curve C). As mentioned in Sec. III, the results of employing a CPM model for the nuclear cascade would give a result between these two curves; we see the experimental data are

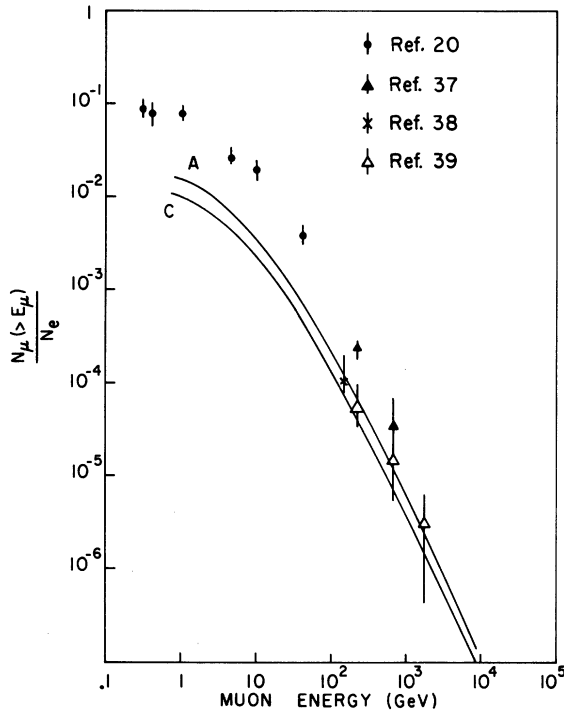


FIG. 4. Ratio of average integral muon number to shower size for showers of fixed size $N_e = 10^6$ vs muon threshold energy. Curve A: calculation with constant cross section and intranuclear cascading. Curve C: constant cross section, nucleon target. The lower-energy data are summarized in Ref. 20.

much higher than the theoretical points.

Next we attempt to take into account rising cross sections. Without a dynamical model for the elementary interaction, we use the same (scaling) number distributions as above and superimpose a rising σ_{p-air} . The fit we use for the rising total p -air cross section is taken directly from the cosmic-ray data of Yodh *et al.*,³ which is in turn consistent with a σ_{p-air} calculated from a $(1ns)^2$ extrapolation of recent ISR measurements of σ_{pp} . (The σ_{p-air} lower bounds are also consistent with, but do not demand, a more rapid increase in σ_{p-air} .) In addition we assume that $\sigma_{\pi-air} \approx 0.7\sigma_{p-air}$ in accordance with observed interaction lengths of hadrons in air. As we mentioned in Sec. III, the nuclear-target number distributions are then virtually unchanged from the constant-cross-section case.

The results of the calculation for the μ/e ratio including both intranuclear cascading and growing cross sections are shown in Fig. 5, together with the $\sigma = \text{const}$, nucleon-target result (lowest curve). Similar results for the size versus depth are shown in Fig. 6. We see that, although the combined effects of increasing cross section and intranuclear cascading give considerable improvement, the calculated results still do not agree with

the data.

One way to attempt to understand this problem is to recall that the region in which there is the least amount of evidence for Feynman scaling is the central region. A preliminary calculation has been done by Gaisser *et al.*⁹ describing the elementary interaction by the Landau hydrodynamical model,²⁸ which has a multiplicity $\sim E^{1/4}$, but which approximately scales in the fragmentation regions. It was found that the improvement over the original scaling model of Ref. 1 was even less than those introduced by the models shown above. This suggests that if the discrepancy is to be explained by a breakdown of Feynman scaling, it will be necessary to have the breakdown occur *in the fragmentation region*, and not simply at $x=0$. The physical reason for this is easy to understand. As long as a few charged hadrons can carry off a large, energy-independent fraction of the incoming energy, the shower cannot develop as quickly as the data indicate it must. This means, as we pointed out in the Introduction, that the resolution of the difficulty may involve some new physical phenomenon occurring at extremely high energies.

There is, however, another possible resolution of the difficulty which does not involve the introduction of new physics at high energies. As we mentioned in the Introduction, that is to assume

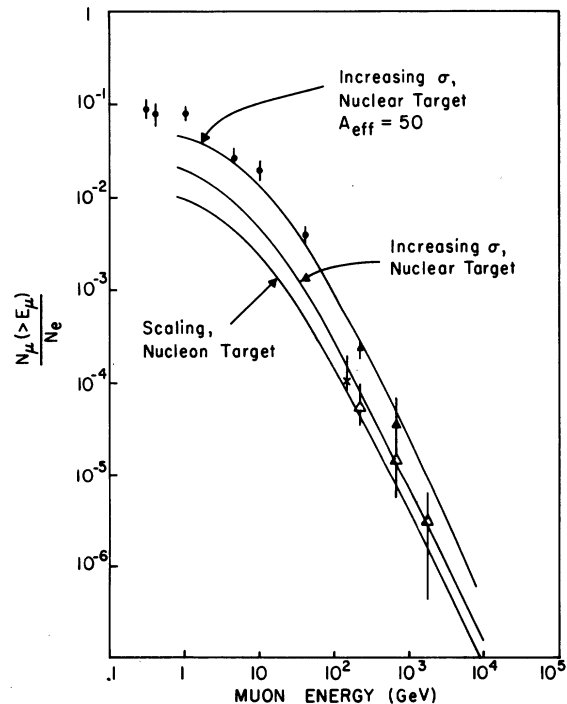


FIG. 5. Ratio of average integral muon number to shower size for showers of fixed size $N_e = 10^6$ vs muon threshold energy. The lowest curve is identical to C of Fig. 4.

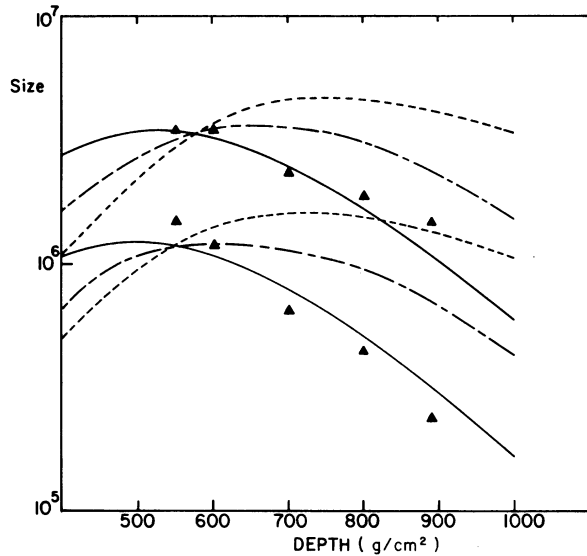


FIG. 6. Shower size vs depth (g/cm^2). Data are from Ref. 22 at primary intensities of 10^{-10} ($\text{cm}^2 \text{ sec sr}^{-1}$) for the lower and 10^{-11} ($\text{cm}^2 \text{ sec sr}^{-1}$) for the upper set. The curves are calculated results, normalized to the data at $\sim 600 \text{ g}/\text{cm}^2$. The short dashed curve is for constant cross section, nucleon target; the dash-dot curve is for increasing cross section plus intranuclear cascading; and the solid curve is for increasing cross section, intranuclear cascading, and $A=50$. The corresponding μ/e curves are shown in Fig. 5.

that the primary cosmic radiation at EAS energies is predominantly heavy nuclei; We can estimate the effect of this hypothesis by assuming that a primary of size A and total energy E is equivalent to A nucleon primaries of energy E/A .

The calculation, then, amounts to adding A independent showers of appropriate energy E/A using the techniques developed in this paper. The results of the calculation, combining the effects of the heavy primary, rising cross sections, and intranuclear cascades are also shown in Figs. 5 and 6. We see that for $A_{\text{eff}} \approx 50$, we can achieve satisfactory agreement with these data.

It has been objected that the assumption of all heavy primaries is inconsistent with observed large fluctuations in EAS properties.^{7,29} We point out, however, that a calculation which takes account of fluctuations in fragmentation of a heavy nucleus in a more realistic way³⁰ leads to larger fluctuations of shower properties than expected on the basis of the pure E/A superposition model,³¹ and that such a calculation has not, to our knowledge, been carried out in a scaling context. Further, it seems plausible that the details of the fragmentation will not affect average shower parameters. It therefore remains possible to account both for average properties and fluctuations with

heavy primaries, though this point remains to be investigated in detail.

The results discussed above and compared with data in Figs. 4, 5, and 6 are for primary energies in the range of several times 10^6 GeV . (The relation between N_e and $\langle E_0 \rangle_{N_e}$ is model-dependent. For showers of fixed size $N_e = 10^6$, $\langle E_0 \rangle_{N_e}$ is $2.4 \times 10^6 \text{ GeV}$ for scaling, $\sigma = \text{const}$, nucleon target; $3.9 \times 10^6 \text{ GeV}$ for increasing σ , nuclear target; and $5.5 \times 10^6 \text{ GeV}$ for $A_{\text{eff}} = 50$, increasing σ , nuclear target.) In view of the discrepancy found it is important to learn at what energies a straightforward extrapolation of $\sim 1000\text{-GeV}$ accelerator data based on Feynman scaling (possibly modified to include increasing cross sections and intranuclear cascading), together with primary spectrum that is mostly protons, begins to fail.

With this in mind we have compared calculations with data³²⁻³⁹ on N_μ/N_e for a range of sizes from $N_e \sim 10^5$ up to $N_e \sim 10^7$. All three models discussed here give $N_\mu \propto N_e^\alpha$, with $\alpha \sim 0.7$ for the whole range, $10^5 < N_e < 10^7$, over which calculations have been made (this corresponds roughly to $3 \times 10^5 \text{ GeV} < \langle E_0 \rangle_{N_e} < 3 \times 10^7 \text{ GeV}$). The data of Refs. 33-35 give $N_\mu \propto N_e^\alpha$, $0.6 \leq \alpha \leq 0.8$ over this same range, with N_μ/N_e consistently higher than the calculation assuming proton primaries, as shown in Figs. 4 and 5 for $N_e = 10^6$. These data cover the muon energy range $1 \leq E_\mu \leq 50 \text{ GeV}$. However, below 10^6 GeV there are the following hints of a qualitative change in the data: The data of Chatterjee *et al.*³⁶ on $N_\mu (> 1 \text{ GeV})$ does show a break around $N_e \sim 10^6$ from $\alpha \sim 0.3$ below to $\alpha \sim 0.8$ above $N_e \sim 10^6$. Furthermore, the most recently reported version of the $E_\mu > 50 \text{ GeV}$ data^{32,38,39} shows $\alpha \sim 0.4$ for $10^5 \leq N_e \leq 3 \times 10^6$ and gives an N_μ/N_e ratio consistent with the proton primary calculations, at $N_e = 10^6$, as shown by the open triangles in Figs. 4 and 5. The earlier interpretation of this data³⁷ gave $\alpha \sim 0.6$ with N_μ/N_e consistent with $A_{\text{eff}} \approx 50$, as shown by the solid triangles in Fig. 5.

In summary, there is no clear evidence for a change in the features of muon and electromagnetic components of air showers for primary energies $\geq 10^6 \text{ GeV}$, and much of the experimental evidence is consistent with no change above a few times 10^5 GeV . Thus, significant changes in the primary composition, or in features of high-energy interactions, or both must occur between 1000 and 10^6 GeV .^{8,40}

There is, unfortunately, a gap in simultaneous measurement of two or more EAS properties between a few times 10^3 GeV , where both the μ and electron components have been detected at ground level by their Čerenkov radiation high in the atmosphere,⁴¹ and $\sim 10^5 \text{ GeV}$, above which conventional EAS techniques are used. We note, however,

that cascades initiated by high-energy primaries will also depend on lower-energy hadronic interactions in the cascade so that properties of hadronic interactions in this intermediate energy range may be elucidated by further studies of conventional EAS properties, including fluctuations, hadrons, and lateral distribution. Resolution of the primary composition question, however, requires observations of primaries in the energy range in question. The underground multiple-muon experiments⁴² and conventional EAS Čerenkov light measurements⁴³ can possibly shed light on these questions in this

intermediate energy range. Simultaneous measurements of several shower properties are, however, desirable.

It is amusing to note that by replotting recent cosmic-ray composition data⁴⁴ versus total energy per nucleus and by extrapolating it over three orders of magnitude to 10^6 GeV, one obtains $A_{\text{eff}} \approx 50$ due to the observed relative flatness of the iron spectrum. In pointing this out we do not wish to imply this possibility to be either more or less likely than the possibility of new physics discussed above.

- *Work supported in part by a Cottrell Research grant, The Research Corporation, and by the National Science Foundation under Grant No. GP-39179.
- †Work supported in part by the National Science Foundation.
- ¹T. K. Gaisser and R. H. Maurer, Phys. Lett. **42B**, 444 (1972).
- ²G. K. Ashley *et al.*, Phys. Rev. Lett. **31**, 1091 (1973).
- ³G. B. Yodh, Yash Pal, and J. S. Trefil, Phys. Rev. Lett. **28**, 1005 (1972); Phys. Rev. D **8**, 3233 (1973).
- ⁴P. Camillo, P. M. Fishbane, and J. S. Trefil, Phys. Rev. D (to be published).
- ⁵T. K. Gaisser and G. B. Yodh, Bartol report, 1973 (unpublished).
- ⁶J. Wdowczyk and A. W. Wolfendale, in *Proceedings of the Thirteenth International Conference on Cosmic Rays, Denver, 1973* (Colorado Associated Univ. Press, Boulder, 1973), Vol. 3, p. 2336.
- ⁷N. N. Kolmykov, Yu. A. Fomin, and G. B. Khristiansen, in *Proceedings of the Thirteenth International Conference on Cosmic Rays, Denver, 1973* (Ref. 6), Vol. 4, p. 2633.
- ⁸S. I. Nikolskii, Zh. Eksp. Teor. Fiz. **51**, 804 (1966) [Sov. Phys.—JETP **24**, 535 (1967)], argued some time ago that EAS data require some such mechanism to set in at $\sim 4 \times 10^4$ GeV.
- ⁹T. K. Gaisser, R. H. Maurer, and C. J. Noble, in *Proceedings of the Thirteenth International Conference on Cosmic Rays, Denver, 1973* (Ref. 6), Vol. 4, p. 2652.
- ¹⁰Bruno Rossi, *High Energy Particles* (Prentice-Hall, New York, 1952), pp. 544–546.
- ¹¹M. Antinucci *et al.*, Nuovo Cimento Lett. **6**, 121 (1973).
- ¹²S. C. Tonwar, S. Naranan, and B. V. Sreekantan, Nuovo Cimento Lett. **1**, 531 (1971).
- ¹³P. K. F. Grieder, in *Proceedings of the Thirteenth International Conference on Cosmic Rays, Denver, 1973* (Ref. 6), Vol. 4, p. 2467.
- ¹⁴T. K. Gaisser and R. H. Maurer, Phys. Rev. Lett. **30**, 1264 (1973).
- ¹⁵W. R. Frazer *et al.*, Phys. Rev. D **5**, 1653 (1972).
- ¹⁶T. K. Gaisser and J. Thornstensen, report (unpublished).
- ¹⁷T. K. Gaisser, J. Geophys. Res. (to be published).
- ¹⁸M. LaPointe, in *Introduction to Experimental Techniques of High Energy Astrophysics*, edited by H. Ögelman and J. R. Wayland (NASA, 1970).
- ¹⁹Yash Pal and B. Peters, K. Dan. Vidensk. Selsk. Mat.-Fys. Medd. **33**, 1 (1964).
- ²⁰J. F. deBeer *et al.*, Proc. Phys. Soc. **89**, 567 (1966).
- ²¹G. Cocconi, Nucl. Phys. **B28**, 341 (1971), and references contained therein.
- ²²H. Bradt *et al.*, in *Proceedings of the Ninth International Conference on Cosmic Rays, 1965*, edited by A. C. Stickland (The Institute of Physics and the Physical Society, London, England, 1966), Vol. 2, p. 715; M. LaPointe *et al.*, Can. J. Phys. **46**, S18 (1968).
- ²³Don M. Tow, Phys. Rev. D **7**, 3535 (1973).
- ²⁴P. M. Fishbane and J. S. Trefil, Phys. Rev. Lett. **31**, 734 (1973).
- ²⁵P. M. Fishbane and J. S. Trefil, Phys. Rev. D **9**, 168 (1974), discuss the CPM picture in detail.
- ²⁶P. M. Fishbane, J. L. Newmeyer, and J. S. Trefil, Phys. Rev. Lett. **29**, 685 (1972); Phys. Rev. D **7**, 3324 (1973).
- ²⁷D. Bogert *et al.*, Phys. Rev. Lett. **31**, 1271 (1973).
- ²⁸P. Carruthers and M. Duong-van, Phys. Rev. D **8**, 859 (1973).
- ²⁹K. Suga *et al.*, Acta Phys. Hungarica **29**, Suppl. 3, 423 (1969), and references quoted therein.
- ³⁰C. J. Waddington and P. S. Freier, in *Proceedings of the Thirteenth International Conference on Cosmic Rays, Denver, 1973* (Ref. 6), Vol. 4, p. 2449.
- ³¹H. E. Dixon *et al.*, in *Proceedings of the Thirteenth International Conference on Cosmic Rays, Denver, 1973* (Ref. 6), Vol. 4, p. 2473.
- ³²K. Sivaprasad, Ph.D. thesis, Bombay, 1971 (unpublished).
- ³³S. N. Vernov *et al.*, Acta Phys. Hungarica **29**, Suppl. 3, 429 (1970).
- ³⁴H. Hasegawa *et al.*, J. Phys. Soc. Japan **17**, Suppl. 3, 189 (1962).
- ³⁵J. C. Earnshaw *et al.*, Can. J. Phys. **46**, S122 (1968).
- ³⁶B. K. Chatterjee *et al.*, Can. J. Phys. **46**, S131 (1968).
- ³⁷B. K. Chatterjee *et al.*, Can. J. Phys. **46**, S13 (1968).
- ³⁸Y. C. Saxena, J. Phys. A **5**, 1502 (1972).
- ³⁹S. Naranan *et al.*, in *Proceedings of the Thirteenth International Conference on Cosmic Rays, Denver, 1973* (Ref. 6), Vol. 3, p. 1872. See also Ref. 32.
- ⁴⁰R. M. Vatcha and B. V. Sreekantan [J. Phys. A **6**, 1050 (1973); A **6**, 1067 (1973); A **6**, 1078 (1973)] have analyzed properties of high-energy hadrons in showers. They find that characteristics of the hadronic component vary for $\langle E_0 \rangle_{N_0} \approx 5 \times 10^5$ GeV, and conclude that a change in primary composition alone cannot account for the observations and that changes in the nuclear

interaction properties must occur.

⁴¹J. E. Grindlay and H. F. Helmken, in *Proceedings of the Thirteenth International Conference on Cosmic Rays, Denver, 1973* (Ref. 6), Vol. 1, p. 202.

⁴²J. W. Elbert *et al.*, in proceedings of the Conference on Particles and Fields, Berkeley, 1973 (to be published).

⁴³See, e.g., C. Gerdes, C. Y. Fan, and T. C. Weekes, in *Proceedings of the Thirteenth International Conference on Cosmic Rays, Denver, 1973* (Ref. 6), Vol. 1, p. 219.

⁴⁴R. Ramaty, V. K. Balasubrahmanyam, and J. F. Ormes, *Science* 180, 731 (1973).